Journal of Applied Remote Sensing

RemoteSensing.SPIEDigitalLibrary.org

Downscaling SMAP and SMOS soil moisture with moderate-resolution imaging spectroradiometer visible and infrared products over southern Arizona

Kyle R. Knipper
Terri S. Hogue
Kristie J. Franz
Russell L. Scott

SPIE.

Kyle R. Knipper, Terri S. Hogue, Kristie J. Franz, Russell L. Scott, "Downscaling SMAP and SMOS soil moisture with moderate-resolution imaging spectroradiometer visible and infrared products over southern Arizona," *J. Appl. Remote Sens.* **11**(2), 026021 (2017), doi: 10.1117/1.JRS.11.026021.

Downscaling SMAP and SMOS soil moisture with moderate-resolution imaging spectroradiometer visible and infrared products over southern Arizona

Kyle R. Knipper,[a,*] Terri S. Hogue,[a] Kristie J. Franz,[b] and Russell L. Scott[c]

[a]Colorado School of Mines, Hydrologic Science and Engineering, Department of Civil and Environmental Engineering, Golden, Colorado, United States

[b]Iowa State University, Department of Geological and Atmospheric Sciences, Ames, Iowa, United States

[c]Southwest Watershed Research Center, USDA-Agricultural Research Services, Tucson, Arizona, United States

Abstract. This current study explores satellite-based soil moisture downscaling approaches and applies them to common passive microwave retrievals. Three variations of a second-order polynomial regression were tested based on the surface temperature/greenness index concept and merged information from higher spatial resolution moderate-resolution imaging spectroradiometer with soil moisture active passive (SMAP) and soil moisture and ocean salinity (SMOS) products to obtain soil moisture estimates at higher resolutions (1 km). Downscaled products were evaluated at the Walnut Gulch Experimental Watershed (WGEW) in southeastern Arizona. Results show slight differences in performance among the three downscaling methods and little improvement between original low-resolution products and downscaled (1 km) products. Spatial analysis over WGEW demonstrates downscaled products were able to decipher small-scale heterogeneities in surface soil moisture, though spatial variability remains low compared to observations with a difference of only 0.06 m^3/m^3 in spatial standard deviation between observations and the mean between downscaling techniques. Results demonstrate the ability of both SMOS and SMAP to represent soil moisture accurately on the point scale without applying downscaling techniques in the region under study. [DOI: 10.1117/1.JRS.11.026021]

Keywords: soil moisture; remote sensing; moderate-resolution imaging spectroradiometer; soil moisture and ocean salinity; soil moisture active passive; downscaling; semiarid; Walnut Gulch Experimental Watershed.

Paper 16676 received Sep. 12, 2016; accepted for publication May 1, 2017; published online May 25, 2017.

1 Introduction

Soil moisture is a critical component of the hydrologic cycle, directly influencing feedbacks between the land and the atmosphere, contributing to regional dynamics of the atmospheric boundary layer, and influencing local to global weather and climate patterns.[1–4] Traditional ground-based measurements provide frequent and accurate estimates of soil moisture, but are incapable of resolving spatial heterogeneities. Alternatively, satellite-based microwave remote sensing techniques can provide large-scale spatially distributed soil moisture estimates with routine frequency.[5,6] These coarse resolution estimates are sufficient when applied on a global scale, but are unrepresentative of the surface heterogeneity found at smaller regional/watershed scales.[7]

Previous studies have demonstrated the utility of microwave sensors for the acquisition of surface soil moisture due to their high sensitivity to changes in near-surface soil moisture at

*Address all correspondence to: Kyle R. Knipper, E-mail: kyleknipper7@gmail.com

frequencies <10 GHz, availability under all-sky conditions, and decreased susceptibility to atmospheric interference.[5,6,8,9] However, an increase in vegetation and surface roughness tends to reduce the sensitivity of microwave observations to soil moisture signals,[10,11] with their effects becoming more pronounced with an increase in microwave frequency.[12] Consequently, frequencies in the L-band (~1 to 2 GHz) are preferred as they are capable of estimating soil moisture over larger ranges of vegetation type and amount and penetrate to a depth of roughly 5 cm.[13,14] Unfortunately, this greater sensitivity to soil moisture subsequently results in lower spatial resolution because of the trade-off between spatial and spectral resolution.

The first L-band satellite dedicated to the global measurement of near-surface soil moisture, the soil moisture and ocean salinity (SMOS) mission,[15,16] was launched by the European Space Agency in November 2009. SMOS provides brightness temperature measurements of the Earth at different polarization and incident angles, as well as derived soil moisture products (~43-km spatial resolution).[17,18] The National Aeronautics and Space Administration's (NASA) soil moisture active passive (SMAP) mission[19] was launched in January 2015 and is the only additional satellite mission dedicated to surface soil moisture observations. SMAP incorporated a radiometer (passive) and radar (active), both operating in the L-band frequency. The spatial resolutions of the radar and radiometer are ~1 km × 1 km and ~39 km × 47 km, respectively. The concept of the SMAP mission was to combine complementary attributes of passive and active observations to obtain soil moisture at a 9-km spatial resolution. However, due to problems with the radar's high power amplifier, the SMAP's radar is no longer able to transmit data, allowing only the passive radiometer data to be available.

The spatial resolutions of SMOS and SMAP are adequate for many global applications, but are coarse and unrepresentative of the surface heterogeneity found at catchment to regional scales.[7] Merlin et al.[20] points out that most hydrological processes are better observed and modeled at scales at or <1 km; hence, there is a need to downscale coarse resolution microwave-based soil moisture products to resolutions necessary for watershed-scale applications and regional decision-making. In this context, several downscaling methods have been proposed, including those based on the use of topography and soil depth,[21] as well as those that use a combination of passive microwave data, fine-scale optical data, and/or surface process models.[22,23] The current study utilizes the triangle/trapezoidal method, which is characterized by the unique relationship among soil moisture availability, land surface temperature (LST), and a vegetation index (VI).[24,25] Utilizing such an approach has three important advantages: (1) requires no ground-based ancillary data, (2) requires no site-specific calibration, and (3) is computationally efficient. As such, the method can be applied in near real time with satellite-derived remote sensing data as its sole input. Several authors have utilized this approach by combining coarse resolution (~25 to 50 km) passive microwave sensor data, such as soil moisture, with high-resolution (1 km) visible/infrared sensor data, such as LST and VI.[12,22,26,27] Additional studies have suggested the addition of albedo or brightness temperature to strengthen the relationship with soil moisture.[22,28] However, prior applications have yet to directly compare differences in downscaling techniques using SMOS and the recently available SMAP soil moisture retrievals.

This study utilizes two passive microwave remote sensor satellites (SMAP and SMOS) and three variations of a second-order polynomial regression formula (based on the triangle method) to test the ability of each satellite and each downscaling method to capture the spatial and temporal heterogeneity of soil moisture over a region in southeastern Arizona. The second-order polynomial regression formula is used to parameterize soil moisture based on the triangle technique relating LST, VI, and/or albedo or brightness temperature. Downscaled soil moisture estimates (1 km) were evaluated at point and spatial scales over a densely instrumented watershed.

2 Study Area

The study area is the Walnut Gulch Experimental Watershed (WGEW) operated by the U.S. Department of Agriculture's Agricultural Research Service and located in semiarid southeastern Arizona (Fig. 1). The WGEW has an area of roughly 148 km^2, with the latitude and longitude ranging from 31.78°N to 31.66°N and from 109.86°W to 110.15°W, respectively. The main land

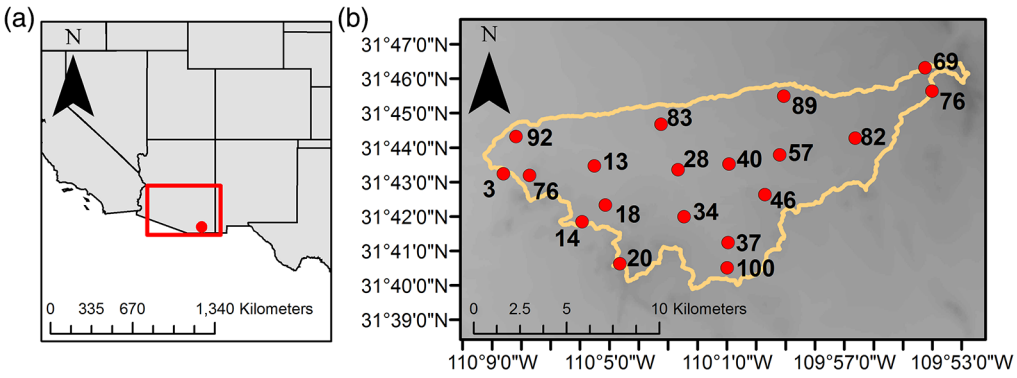

Fig. 1 DEM of the WGEW and 19 of the surface soil moisture sensors. (a) and (b) The red box outlines the domain used in the linking model to merge information from coarse resolution soil moisture satellites and higher resolution LST/EVI parameters.

cover type is predominantly shrublands and grasslands (97%) with areas of developed open space (2%).[29] Soils are mainly sands and gravel with good drainage.[30] The climate is classified as semiarid, with over half of the total rainfall occurring between July and September during the North American monsoon (NAM).[31] Precipitation during the NAM is characterized by local, short-duration, high-intensity convective thunderstorms, which heavily influence ecosystem response and surface soil moisture variability.[12,32–35] The region outlined in red [Fig. 1(a)] is the domain used in the linking model to merge information from coarse resolution and higher resolution products. A large domain is required to satisfy the constraint of requiring warm and cold pixels in each scene.

The distributed soil moisture network [Fig. 1(b)] was used for initial validation. This network has been in operation since 2002 and has been used in the validation of advanced microwave scanning radiometer-earth observing system products,[36] aquarius,[37] advanced scatterometer,[38] and SMOS products.[39] All probes (Stevens Hydra Probes) are installed horizontally at a depth of 5 cm with an effective sensing range of 3 to 7 cm from the surface and record hourly instantaneous data. Measurements of soil moisture were averaged between 5:00 a.m. and 7:00 a.m. to match satellite overpass times. The period of study for the current investigation is from April 1, 2015 to October 4, 2016.

3 Datasets

3.1 *Satellite Observations (SMOS, SMAP, and MODIS)*

3.1.1 *Soil moisture and ocean salinity satellite observations*

The SMOS level 3 (L3) soil moisture products were used in this study. Associated brightness temperature estimates are also included in the L3 product. SMOS L3 soil moisture products were created through the algorithm for retrieving soil moisture from brightness temperature from the L2 retrieval algorithm,[17,40] the best estimation of soil moisture and dielectric constant based on a minimization of a data quality index, as well as through temporal and/or spatial resampling or processing [Centre Aval de Traitement des Donnees SMOS (CATDS)]. This resampling or processing creates a soil moisture product on a 25-km spatial resolution grid with a target accuracy similar to the L2 product (0.04 m^3/m^3 at spatial resolution <50 km).[17] SMOS has a sun-synchronous orbit with local equatorial crossing times of ~6:00 a.m. and 6:00 p.m. in ascending and descending nodes, respectively.[17] Only ascending (6:00 a.m.) SMOS data were used in this study as it is expected that surface soil conditions will generally be closest to thermal equilibrium and uniformity at this time.[16,19,41] SMOS soil moisture data are discarded when the probability of radio-frequency interference is high, the quality of retrieval is poor (DQX > 0.07), the soil moisture value is negative, or the retrieval has failed.

3.1.2 *Soil moisture active passive satellite observations*

The SMAP L3 product (L3_SM_P) is used in the current study. Associated brightness temperature estimates are also included in the L3 product. The L3 product is a daily global composite of the Level 2 surface soil moisture data and is available at 40-km resolution output on a fixed 36-km updated equal-area scalable Earth-2 projection.[19] SMAP has a sun-synchronous orbit with a local time of ascending and descending nodes of 6:00 p.m. and 6:00 a.m., respectively. Due to an expectation of thermal equilibrium and uniformity of surface soil conditions, as mentioned for SMOS, only descending (6:00 a.m.) SMAP soil moisture data are used in the current study.

3.1.3 *Moderate-resolution imaging spectroradiometer observations*

Utilized MODIS products include the version 5 MODIS aqua 1-km resolution daily nighttime LST product (MYD11A1), version 5 MODIS terra/aqua 1-km resolution 16-day composite EVI product (MYD13A2/MOD13A2), and version 5 MODIS terra/aqua 1-km resolution 8-day composite Albedo product (MCD43B3). Due to the optimization of the enhanced vegetation index (EVI) in improving the vegetation signal and reducing soil background influence,[42] EVI was utilized rather than the normalized difference vegetation index. The phasing of both terra and aqua EVI products generates a combined 8-day time series of vegetation indices. All MODIS products are acquired from the NASA Reverb ECHO site in the standard hierarchical data format for the time period under investigation.

4 Downscaling Methodology

Several theoretical and experimental studies have demonstrated the unique relationship among soil moisture availability, LST, and vegetation indices.[22,24,26,27] This relationship can be expressed through a second-order polynomial regression formula, used in conjunction with high-resolution EVI and LST, to obtain higher resolution soil moisture estimates. The regression relation, proposed by Carlson et al.,[24] can be written as

$$\mathrm{SM} = \sum_{i=0}^{i=\mathrm{n}} \sum_{j=0}^{j=n} a_{ij} \mathrm{EVI}^{*i} \mathrm{LST}^{*j}, \tag{1}$$

where n is the order of the model and is typically chosen as two for computational efficiency.[28,43] SM is the estimated soil moisture, and EVI^* and LST^* are the normalized EVI and normalized observed LST, respectively, defined as

$$\mathrm{EVI}^* = \frac{\mathrm{EVI} - \mathrm{EVI}_{\min}}{\mathrm{EVI}_{\max} - \mathrm{EVI}_{\min}}, \tag{2}$$

$$\mathrm{LST}^* = \frac{\mathrm{LST} - \mathrm{LST}_{\min}}{\mathrm{LST}_{\max} - \mathrm{LST}_{\min}}, \tag{3}$$

where $\mathrm{EVI}_{\min}$ and $\mathrm{EVI}_{\max}$ are the minimum and maximum MODIS-derived EVI values determined over the study domain, and $\mathrm{LST}_{\min}$ and $\mathrm{LST}_{\max}$ are the minimum and maximum MODIS-derived LST values determined over the study domain. Regression coefficients (a_{ij}) are determined by replacing SM in Eq. (1) with coarse scale SMOS (25 km) or coarse scale SMAP (36 km) soil moisture estimates and resampling EVI and LST to match the corresponding satellite product spatial resolution. Next, the system of linear equations for all the pixels in the image is solved to obtain the regression coefficients (a_{ij})—which are specific for each day and scene being analyzed. It is important to note that LST and EVI at low (25 or 36 km) and high (1 km) spatial resolution are computed so as to have the same mean value within each coarse scale pixel, ensuring that the downscaled product has the same mean as the 25-km SMOS or 36- km SMAP soil moisture product. Estimated regression coefficients corresponding to SMOS or SMAP are then utilized to estimate a MODIS-scale (1 km) soil moisture estimate. This approach [Eq. (1)] is referred to as downscaling method 1 (DS1) in the evaluations.

A similar approach was proposed by Piles et al.[28] and introduces the use of brightness temperature to the regression formula in an attempt to strengthen the relationship between land surface parameters and soil moisture. This modified regression formula is written as

$$\mathrm{SM} = \sum_{i=0}^{i=n} \sum_{j=0}^{j=n} \sum_{k=0}^{k=n} a_{ijk} \mathrm{EVI}^{*i} T_s^{*j} T_b^{*k}, \tag{4}$$

with T_b defined as

$$T_b^* = \frac{T_b - T_{b_{\min}}}{T_{b_{\max}} - T_{b_{\min}}}, \tag{5}$$

where $T_{b,\min}$ and $T_{b,\max}$ are the minimum and maximum SMOS- or SMAP-observed brightness temperature values determined over the study domain. This approach is referred to as downscaling method 2 in the evaluations (DS2). In addition to the aforementioned approaches, Chauhan et al.[22] introduce MODIS albedo data (α) into the regression formula and can be written as

$$\mathrm{SM} = \sum_{i=0}^{i=n} \sum_{j=0}^{j=n} \sum_{k=0}^{k=n} a_{ijk} \mathrm{EVI}^{*i} T_s^{*j} \alpha^{*k}, \tag{6}$$

with α^* defined as

$$\alpha^* = \frac{\alpha - \alpha_{\min}}{\alpha_{\max} - \alpha_{\min}}, \tag{7}$$

where $\alpha_{\min}$ and $\alpha_{\max}$ are the minimum and maximum MODIS-derived albedo values determined over the study domain. Equation (6) is noted as downscaling method 3 in the evaluations (DS3). All three downscaling methods were solved in the same manner for both SMOS and SMAP coarse scale soil moisture estimates.

It is important to note limitations when using MODIS visible/infrared data for downscaling both SMOS and SMAP soil moisture data. First, the sensing depths for SMOS and SMAP L-band (~1.4 GHz) for bare soil are ~5 cm. Sensing depth for the MODIS thermal infrared band is ~1 mm (skin). The thermal regime in the 0- to 5-cm profile is likely to be very different from that of 0 to 1 mm, where more rapid fluctuations are likely and increased correlation to ambient temperatures may lead to misrepresentation of spatial and temporal variability of the underlying soil layer. The thermal regime in the 0- to 5-cm profile is also likely to differ from ground observations (~2.5 to 7.5 cm), with an expected low bias due to rapid drying of the top surface soil layer. Furthermore, L-band is capable of penetrating moderately vegetated regions, where thermal infrared is unable to sense through a vegetation layer.

5 Methodology

Analysis performed in the current study involved both a qualitative assessment of surface soil moisture maps and spatial and temporal statistical evaluation. Statistical evaluation was done through a comparison between original SMOS and SMAP soil moisture products and each subsequently derived downscaled soil moisture product (DS1, DS2, and DS3). Evaluation of the spatial domain was included to determine the degree of success of the disaggregation techniques for SMOS and SMAP as the aim of each technique is to improve the spatial representation. Standard statistical metrics include correlation (R), coefficient of determination (R^2), slope, and bias. In addition, the standard deviation of the error was included [Eq. (8)],[44,45] which is not compromised by the bias in the mean and amplitude of the time series that affects the root-mean-square deviation (RMSD).[30] This metric will be referred to as unbiased-RMSD or ubRMSD[46] as in Morelo et al.[30]

$$\mathrm{ubRMSE} = \sqrt{E\{[(\mathrm{SM}_{\mathrm{satellite}} - E\{\mathrm{SM}_{\mathrm{satellite}}\}) - (\mathrm{SM}_{\mathrm{in\ situ}} - E\{\mathrm{SM}_{\mathrm{in\ situ}}\})]^2\}}, \tag{8}$$

where $E\{\}$ is the expectation operator, and $\mathrm{SM}_{\mathrm{satellite}}$ and $\mathrm{SM}_{\mathrm{in\ situ}}$ are the satellite and *in situ* soil moisture time series, respectively. Spatial statistical analysis consists of computing the statistical

metric between the satellite and *in situ* values for each day before deriving the average of each metric for the whole period. Temporal statistical analysis consists of computing the statistical metric for each site through the entire time period before taking the average among all sites.

6 Results and Discussion

6.1 *Spatial Evaluation*

In order to determine the success of each downscaling technique, a statistical analysis on the *in situ* soil moisture data over WGEW was conducted first. Temporal and spatial variability of *in situ* soil moisture observations were analyzed by evaluating the distribution of spatial standard deviation (spatial σ), temporal standard deviation (temporal σ), and average soil moisture values (Fig. 2). Spatial σ [Fig. 2(a)] is the standard deviation of the soil moisture distribution on each day. Temporal σ [Fig. 2(b)] is the standard deviation of the soil moisture time series of each site.

In situ soil moisture values show a narrow distribution of spatial σ, with a mean value of $\sim$0.03 m^3/m^3 [Fig. 2(a)], indicating little spatial variability throughout the study period at WGEW. Temporal σ shows a slightly larger mean ($\sim$0.05 m^3/m^3), with a similar narrow distribution centered on 0.04 m^3/m^3. Despite the cluster centered on lower temporal σ values, larger temporal σ values are recorded at $\sim$10% of the sites. The soil moisture distribution [Fig. 2(c)] is relatively uniform over the watershed, with values ranging between 0.03 and 0.13 m^3/m^3 and no one value accounting for a majority of the samples.

Satellite-derived soil moisture distributions are much narrower for both original (not downscaled) low-resolution SMOS and SMAP products (top left and bottom left, respectively, Fig. 3). This is expected given the spatial extent of each low-resolution pixel over WGEW. SMOS downscaled soil moisture products 1, 2, and 3 (DS1, DS2, and DS3) (top row, Fig. 3) show slightly wider distributions over the watershed, with DS2 showing the most spatial variability. Conversely, SMAP downscaled soil moisture products 1, 2, and 3 (DS1, DS2, and DS3) (bottom row, Fig. 3) indicate little improvement in the spatial distribution of soil moisture compared with the original low-resolution SMAP soil moisture estimates (bottom left, Fig. 3). Mean (solid line) and median (dashed line) remain consistent with original low-resolution SMOS and SMAP soil moisture observations, indicating downscaled soil moisture estimates remain similar to low-resolution estimates despite their derivation from LST, EVI, and/or T_B and Alb. Analysis shows SMOS DS2, which utilizes T_B in its downscaling approach, provides the greatest amount of spatial variability in soil moisture, with DS1 method showing a narrow distribution.

Figures 4 and 5 contain sample output of all three downscaling methods for both SMOS (top row, Figs. 4 and 5) and SMAP (bottom row, Figs. 4 and 5) on the cloud-free acquisition date of August 18, 2015 (Fig. 4) and September 18, 2016 (Fig. 5). Also included in Figs. 4 and 5 are the original low-resolution SMOS (top, left, Figs. 4 and 5) and SMAP (bottom, left, Figs. 4 and 5)

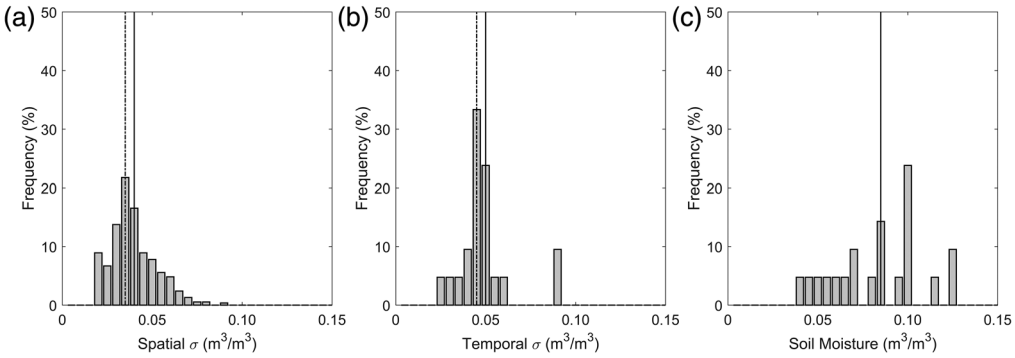

Fig. 2 Distribution of (a) spatial, (b) temporal standard deviations, and (c) soil moisture values for the *in situ* observations of WGEW at the SMOS and SMAP overpass times between April 1, 2015, and October 4, 2016. The median of the distributions is depicted in the dashed line and the mean in the solid line.

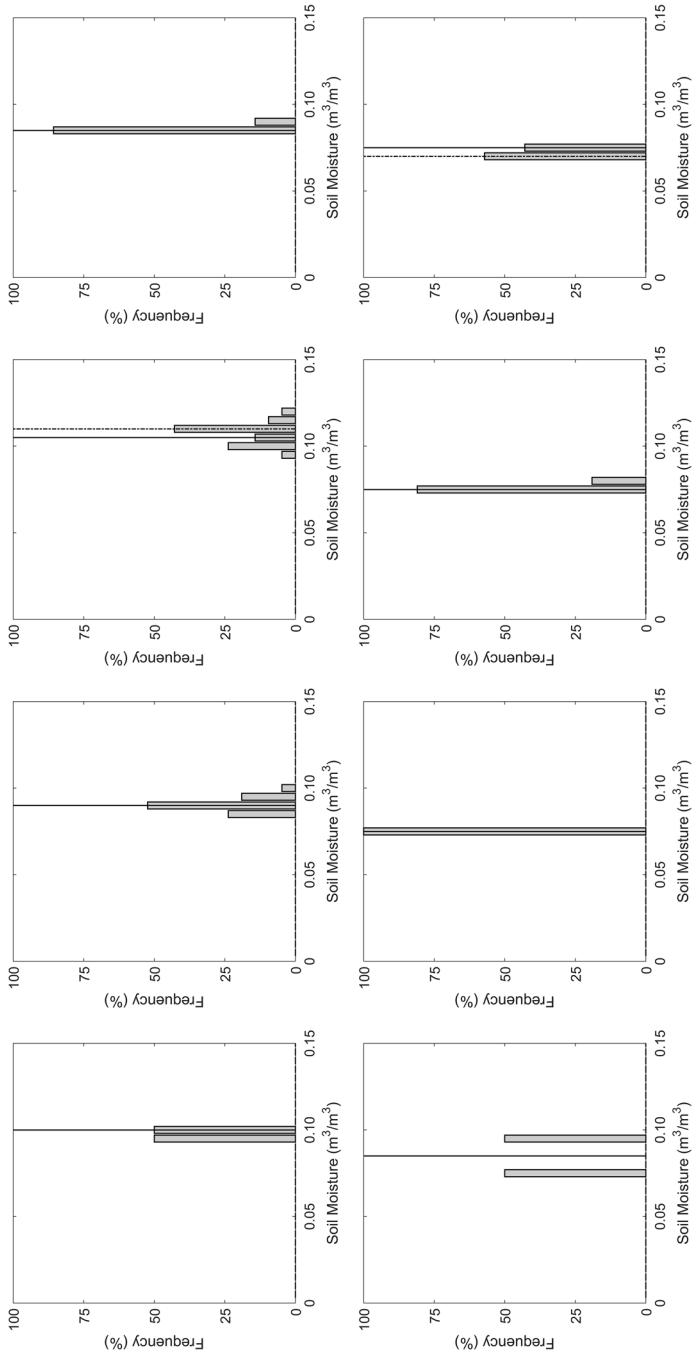

Fig. 3 Distribution of soil moisture values for original, DS1, DS2, and DS3 from SMOS (top, left to right) and SMAP (bottom, left to right) for WGEW over the time period. The median of the distributions is depicted in the dashed line and the mean in the solid line.

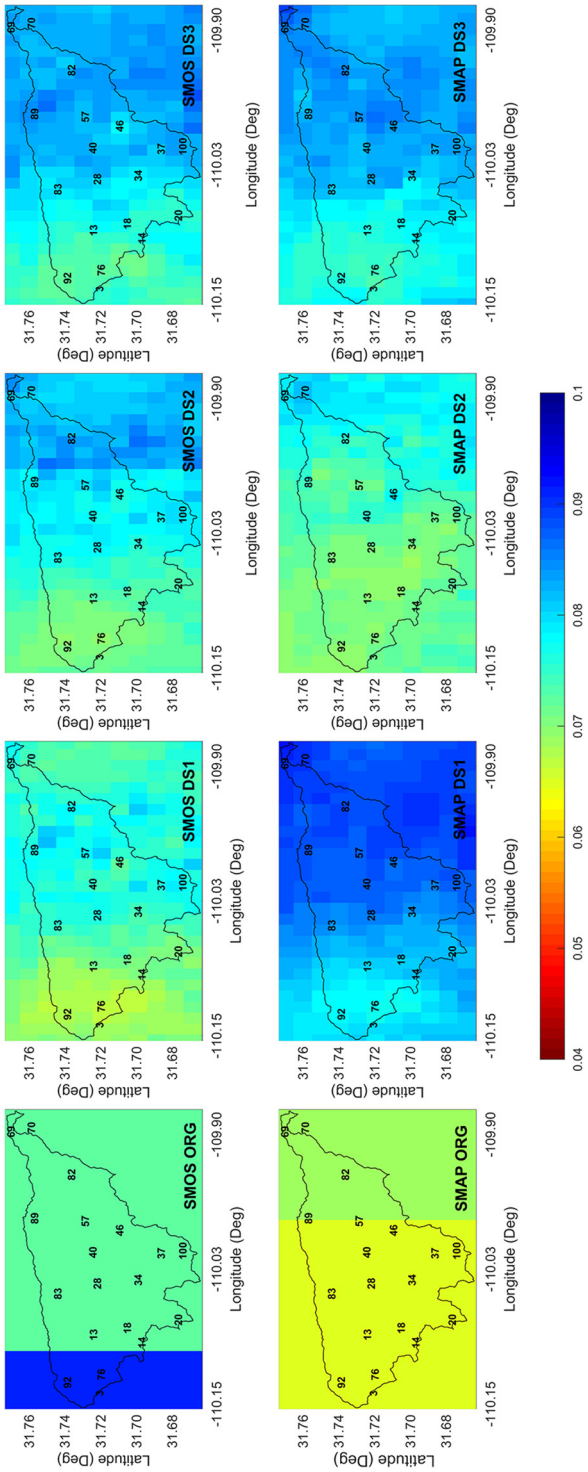

Fig. 4 Maps of soil moisture estimates (m^3/m^3) for original, DS1, DS2, and DS3 SMOS (top, left to right) and SMAP (bottom, left to right) for WGEW on August 18, 2015.

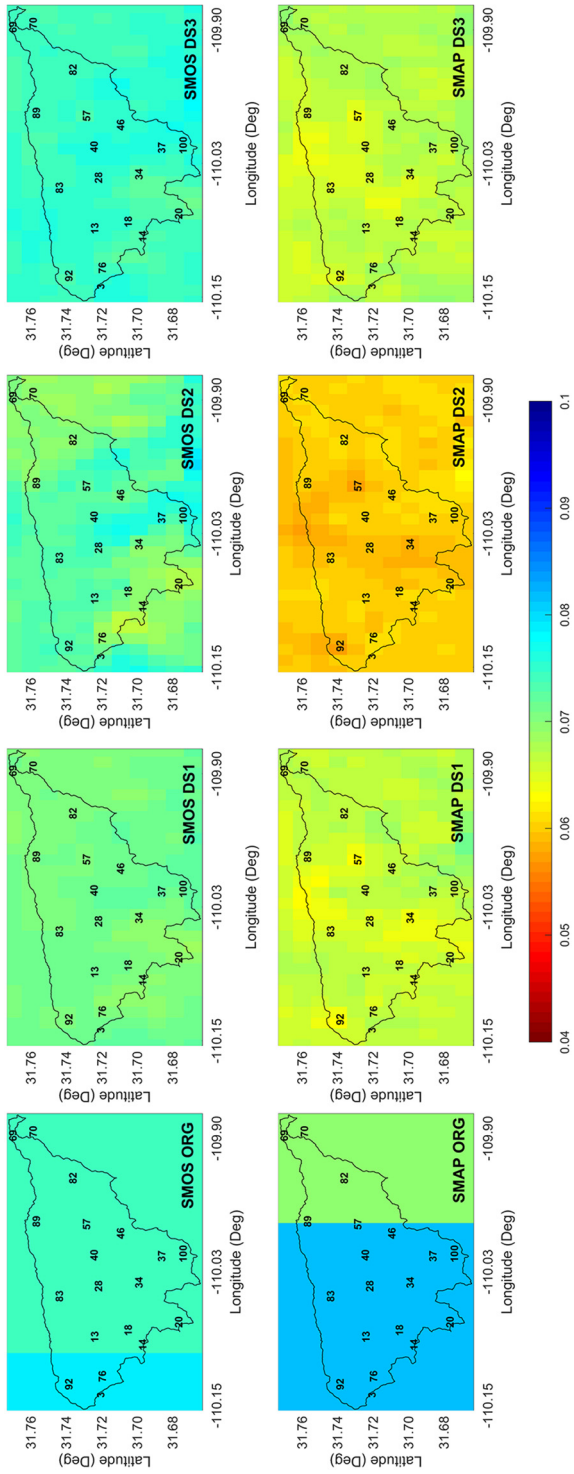

Fig. 5 Maps of soil moisture estimates (m^3/m^3) for original, DS1, DS2, and DS3 SMOS (top, left to right) and SMAP (bottom, left to right) for WGEW on September 18, 2016.

soil moisture estimates for the same date. Qualitative assessment of the disaggregated soil moisture through each individual downscaling method indicates that the downscaling methods are able to capture spatial discrepancies in soil moisture not available in the low-resolution original products (Figs. 4 and 5). Lower soil moisture estimates are reported in the western region of the watershed for both SMOS (top row, Fig. 4) and SMAP (bottom row, Fig. 4) downscaled products on August 18, 2015, while a more uniform distribution of soil moisture is reported on September 18, 2016. The introduction of brightness temperature for the downscaling of SMAP (SMAP DS2) allows surface soil moisture estimates to better match those of the original SMAP pixels on August 18, 2015, while SMAP DS1 and DS3 tend to report values slightly larger as a whole across WGEW. Regardless of the magnitude, spatial patterns among the three remain consistent, with SMAP DS2 showing slightly lower surface soil moisture values over a larger portion of WGEW on both dates. Very little difference in magnitude and spatial variability is reported among SMOS downscaling methods, with SMOS DS1 reporting the lowest soil moisture estimates and SMOS DS3 the highest on average over the entire WGEW region on both dates.

Figure 6 shows observed surface soil moisture estimates made at each site on the same dates, August 18, 2015, and September 18, 2016, with areas among sites filled using inverse distance weighting in order to identify the spatial distribution of observed soil moisture. Observed soil moisture distribution indicates a relatively similar pattern of soil moisture on August 18, 2015, with mainly lower surface soil moisture values in the western region of the watershed [Fig. 6(a)]. Discrepancies between observed and downscaled soil moisture occur at site 13, where the observed value is larger than the surrounding surface soil moisture observations. The observed soil moisture distribution indicates no similarities to downscaled estimates on September 18, 2016. Observed estimates of soil moisture report much lower values in the south central region of the watershed. This spatial variability is not captured in the downscaled estimates, where values are homogeneous across the watershed for all downscaling methods. It is important to

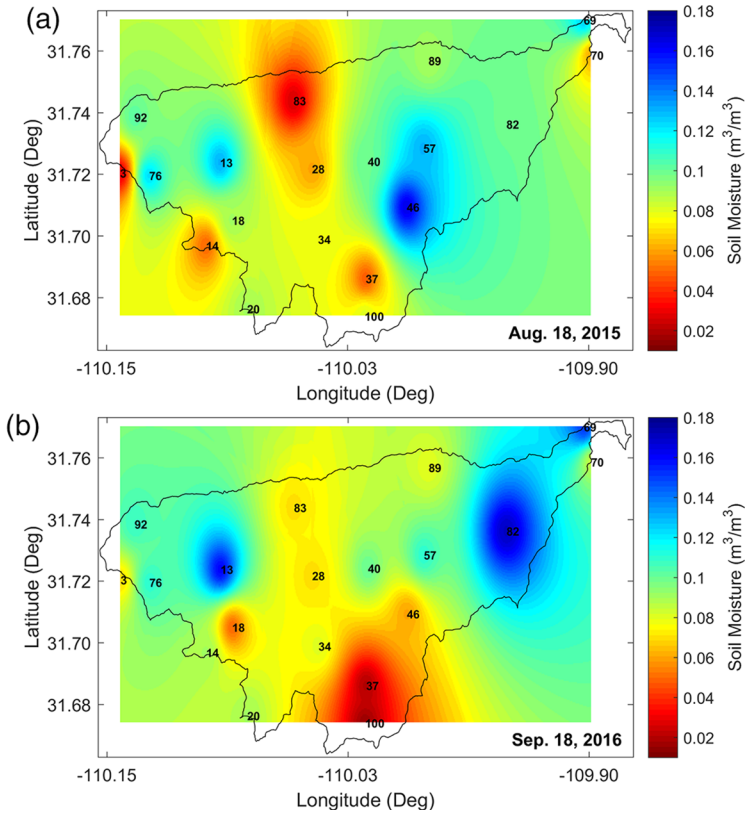

Fig. 6 Map of observed soil moisture estimates (m^3/m^3) for WGEW on (a) August 18, 2015, and (b) September 18, 2016. Data between sites were estimated using inverse distance weighting.

Table 1 Spatial comparison of soil moisture observations with downscaled products over the study period. "DS1," "DS2," and "DS3" refer to downscaled soil moisture obtained through downscaling methods 1, 2, and 3, respectively. All values are expressed in m^3/m^3, except for R and R^2, which are unitless.

	SMOS			SMAP		
	DS1	DS2	DS3	DS1	DS2	DS3
Slope	0.005	0.003	0.003	0.000	0.008	0.004
R^2	0.067	0.079	0.069	0.070	0.078	0.078
R	0.259	0.282	0.262	0.265	0.280	0.280
Bias	0.005	0.010	0.009	0.000	−0.002	−0.003
ubRMSD	0.033	0.033	0.033	0.054	0.054	0.054

note that while spatial patterns between observed soil moisture and downscaled soil moisture are relatively similar on August 18, 2015, differences in spatial σ are large, with observed soil moisture reporting a much larger spatial distribution compared with satellite-derived downscaled estimates. This follows annual spatial analysis, where a much larger spatial distribution for observed compared with satellite-derived downscaled products is reported (Figs. 2 and 3).

Table 1 summarizes the comparison of observations with each downscaling method over the period of study. When comparing the statistics obtained for each downscaled product, it is noted that there is little difference among disaggregation techniques for all statistical metrics. Slope estimates range between 0.003 and 0.005 for downscaled SMOS and 0.000 to 0.008 for SMAP, with R values between 0.259 and 0.282 for downscaled SMOS and 0.265 to 0.280 for downscaled SMAP. Unbiased RMSD (ubRMSD) values remain unchanged among the downscaling techniques, with slightly larger values reported for SMOS. Small differences among variations of downscaling techniques indicate that the addition of albedo or brightness temperature does little to improve the downscaled soil moisture estimates in this region. This reflects results reported by Kim and Hogue,[12] where MODIS LST/EVI were shown to have the strongest spatial correlations to soil moisture in the same region.

Statistical metrics reported here are similar to those in Morelo et al.,[30] where low-resolution SMOS soil moisture estimates were disaggregated over WGEW using a disaggregation algorithm called disaggregation based on physical and theoretical scale change.[47–49] Slope, R, bias, and ubRMSD were reported in the study as 0.110, 0.102, 0.026 m^3/m^3, and 0.037 m^3/m^3, respectively. Moreover, the AACES-I campaign,[48] which took place in southeastern Australia and also validated downscaled soil moisture estimates, report negative correlation values for dates associated with very dry homogeneous soil moisture scenes.[48] This coincides with findings reported here, where minimal spatial variability (i.e., homogeneous surface) and dry conditions lead to unsatisfactory statistical representation.

Additionally, it is important to take into consideration the differences between the validation extent and the SMAP and SMOS resolution. WGEW covers only part of the surface of one SMOS and SMAP pixel. Therefore, the distribution of spatial σ may not be representative of the surface. Moreover, the soils of WGEW are characteristic of rapid infiltration and exfiltration (sands and gravels), reducing the apparent soil moisture spatial contrast at satellite overpass times. These spatial contrasts are a necessary condition for an accurate computation of the downscaling coefficient.

6.2 *Temporal Evaluation*

Temporal evaluation was undertaken for the same period and datasets as Sec. 6.1. Temporal statistics were derived by computing each metric over the time period for each individual site. Values were then averaged over the region. Table 2 displays temporal statistics for WGEW between April 1, 2015, and October 4, 2016. In the case of slope, all downscaled soil moisture measures show degraded values, with slopes decreasing by 0.365 and 0.554 on average between

Table 2 Temporal comparison of soil moisture observations with downscaled products over the study period. "LR" refers to the low-resolution (original) soil moisture product prior to downscaling. "DS1," "DS2," and "DS3" refer to high-resolution soil moisture obtained through downscaling methods 1, 2, and 3, respectively. All values are expressed in m^3/m^3, except for R and R^2, which are unitless.

	SMOS				SMAP			
	LR	DS1	DS2	DS3	LR	DS1	DS2	DS3
Slope	0.958	0.546	0.558	0.675	0.836	0.397	0.406	0.440
R^2	0.372	0.314	0.311	0.323	0.523	0.388	0.352	0.368
R	0.610	0.561	0.558	0.568	0.723	0.623	0.593	0.607
Bias	0.019	0.008	0.013	0.012	0.001	0.002	0.000	−0.002
ubRMSD	0.050	0.042	0.043	0.046	0.032	0.036	0.037	0.037

downscaling methods for SMOS and SMAP, respectively. Similar to Morelo et al.,[30] downscaling slightly degrades R, with values decreasing more drastically for SMAP (−0.115 on average between downscaling methods) than SMOS (−0.048 on average between downscaling methods). Bias and ubRMSD show improvement after disaggregation for SMOS soil moisture estimates, with values remaining similar or slightly worse for downscaled SMAP soil moisture estimates [Table (2)]. Despite improved or worse statistical metrics between downscaled and original low-resolution soil moisture values, little difference is reported between individual downscaling methods for SMOS and SMAP. This coincides with results presented in Sec. 6.1.

Differences between original SMOS and SMAP and corresponding downscaled products can be more easily interpreted through qualitative inspection of scatter plots (Fig. 7) and time series (Fig. 8). Distribution of surface soil moisture appears closer and more symmetric around the 1 : 1 line for both original SMOS and SMAP estimates when compared with downscaled estimates (Fig. 7). Regarding both SMOS and SMAP, the scatter plots show no major differences in downscaling methods, as described statistically in Table 2. This is further elaborated when comparing a time series of estimated soil moisture for each downscaling method at each site (Fig. 8). Although small differences are present, little to no difference is reported among the downscaling

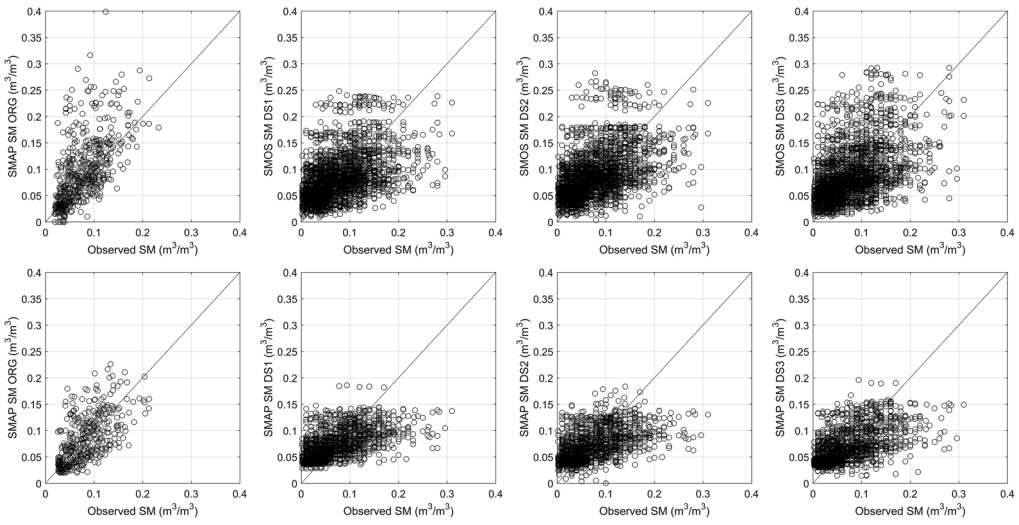

Fig. 7 Scatter plots of original SMOS (top, left), original SMAP (bottom, left), and corresponding downscaled soil moisture through methods DS1, DS2, and DS3 (left to right, respectively) versus *in situ* measurements for all sites within WGEW. The samples here correspond to the period April 1, 2015, to October 4, 2016. Solid line represents the 1 : 1 slope.

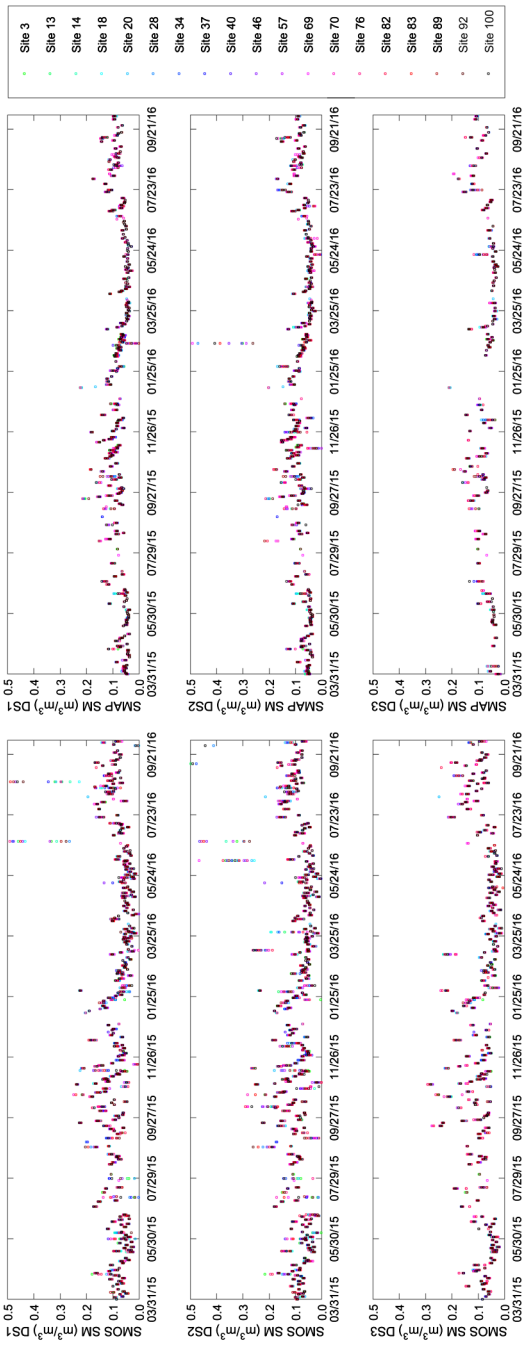

Fig. 8 Time series of downscaled soil moisture (m^3/m^3) reported for SMOS DS1 (top, left), DS2 (middle, left), DS3 (bottom, left) and SMAP DS1 (top, right), DS2 (middle, right), and DS3 (bottom, right) for all sites between April 1, 2015, and October 4, 2016.

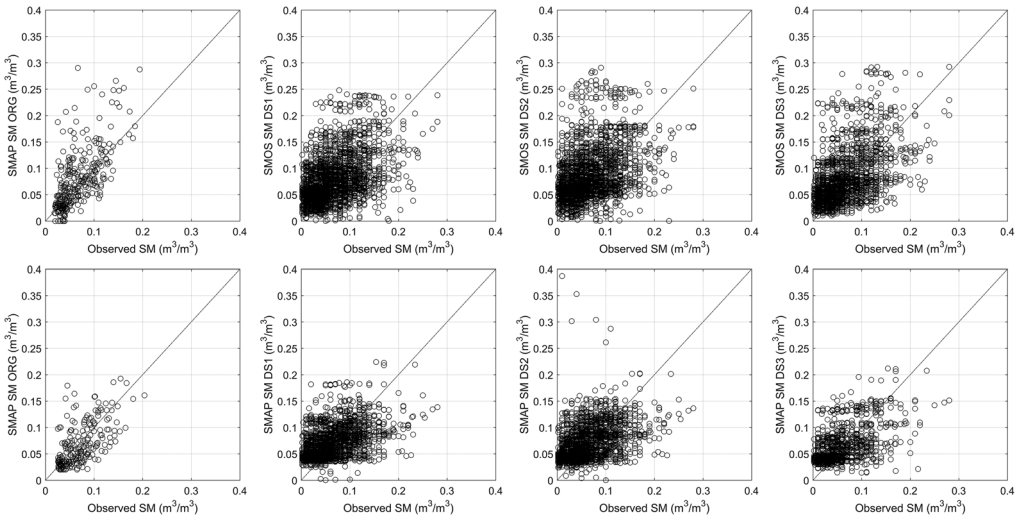

Fig. 9 Scatter plots of original SMOS (top, left), original SMAP (bottom, left), and corresponding downscaled soil moisture through methods DS1, DS2, and DS3 (left to right, respectively) versus *in situ* measurements for all sites within WGEW. The samples here correspond to the nonmonsoon period (not including months June through September). Solid line represents the 1:1 slope.

methods, with magnitudes and spatial distributions remaining similar throughout, as mentioned above.

While interpreting samples during the nonmonsoon periods (not including months June through September), drier conditions lead to disaggregation values that are slightly closer to *in situ* estimates and become more equally distributed around the 1:1 line (Fig. 9). Comparison between the two time series shows an increase in slope for both SMOS and SMAP (+0.034 and +0.021 on average, respectively) when excluding the monsoon season. Correlations remain similar with less than a ±0.04 change in correlation between SMOS and SMAP on average among the downscaling techniques. Versions of the downscaling techniques presented in the current study do not operate as effectively in wet conditions,

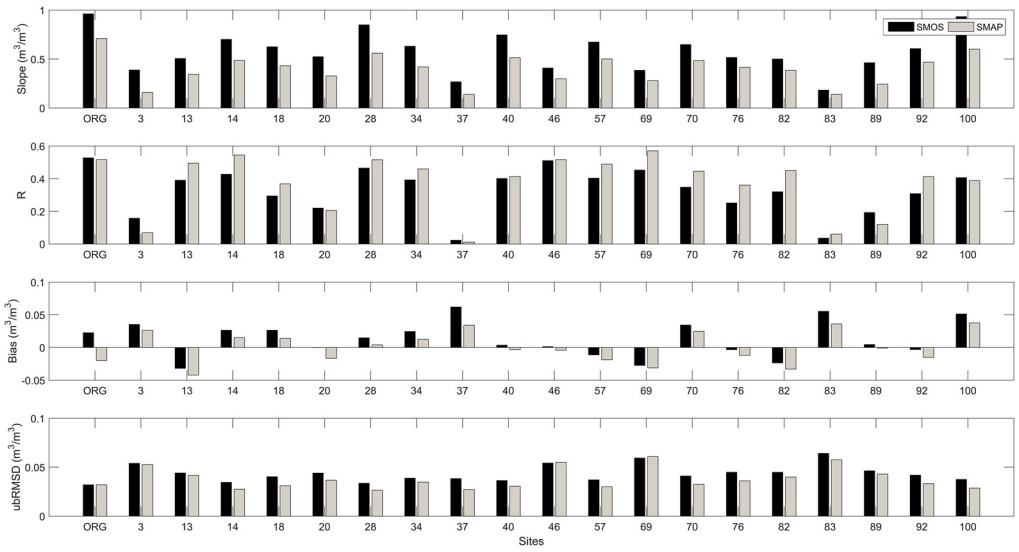

Fig. 10 Bar plots of the statistical metrics such as slope, R, bias, and ubRMSD (top to bottom) for ORG (original low-resolution SMOS/SMAP compared with basin averaged observed soil moisture estimates) and corresponding individual sites for both SMOS and SMAP products. Statistical metrics reported for each individual site are the mean between DS1, DS2, and DS3 due to the small differences reported among the downscaling techniques.

where parameters such as MODIS LST are generally disconnected from soil moisture. This disconnection or decoupling is due to a transition from moisture limited to energy limited conditions.

Site-specific analysis reveals slight differences between ORG statistical metrics (original low-resolution SMOS/SMAP compared with basin averaged observed soil moisture estimates) and corresponding metrics derived at each individual site (average of DS1, DS2, and DS3) (Fig. 10). In regards to slope, all sites (with the exception of 92 and 100) show a decrease in value following disaggregation, with SMAP reporting lower slope values than SMOS at all sites under investigation. R values vary considerably among sites, with the lowest values observed at sites 37 and 83. In contrast to slope, SMAP shows larger R values among all sites on average when compared to SMOS (Fig. 10). Bias values also vary among sites, with larger positive bias values reported at sites 37, 83, and 100 and more negative bias's reported at sites 13, 69, and 82. Values of ubRMSD show less variability among sites, with no significant improvement over the coarse resolution SMOS and SMAP. Site-specific analysis further proves, statistically, little improvement or benefit in downscaling original low-resolution SMOS and/or SMAP in the region under investigation. As such, the importance of qualitative assessment of surface maps, where differences in spatial heterogeneity of surface soil moisture between low- and high-resolution products is apparent, cannot be overstated.

7 Conclusions

In this current study, two passive microwave sensor satellites (SMAP and SMOS) and three variations of a second-order polynomial regression formula were tested to determine the ability of each satellite and each downscaling method to capture the spatial and temporal heterogeneity of soil moisture over WGEW. Variations of the downscaling method were chosen as they are computationally efficient, require no ground-based ancillary data sources, and require no site/region-specific calibration, allowing each to be implemented in near-real time. Each combination of satellite and downscaling method was evaluated over the WGEW and its high-density network of soil moisture sensors between the dates of April 1, 2015 and October 4, 2016.

Overall, SMOS- and SMAP-derived soil moisture estimates under each downscaling method show little variation among methods, indicating the addition of albedo or brightness temperature does little to improve downscaled surface soil moisture estimates. Spatial and temporal statistics indicate modest enhancement in downscaling original low-resolution SMOS and/or SMAP in the region under investigation. Visual assessment of downscaled soil moisture maps for both SMOS and SMAP show that each disaggregation is capable of revealing spatial discrepancies and heterogeneity of the surface. However, these spatial discrepancies and heterogeneity of the surface do not always correspond to observations. Disaggregation techniques applied to SMAP do little to improve the representation of spatial variability in soil moisture, with soil moisture values remaining within bounds set by the original low-resolution product. Lack of improved spatial representation of surface soil moisture following each downscaling procedure is likely associated with a combination of regional characteristics. For example, soils of WGEW and the surrounding region are noted to have high infiltration/exfiltration rates, reducing the apparent soil moisture spatial contrast during satellite overpass times. These spatial contrasts are a necessary condition for accurately downscaling low-resolution soil moisture products. Moreover, downscaling techniques presented here do not operate as sufficiently in increased wet conditions due to a decoupling of satellite derived parameters (LST) and surface soil moisture from a transition from moisture limited to energy-limited conditions.

Key limitations when applying this approach are that the developed downscaled soil moisture estimates are available only during clear-sky days due to the need for MODIS products for the downscaling method. However, because SMOS and SMAP report little to no variability among downscaling methods, it may be possible to supplement original low-resolution SMOS and SMAP soil moisture estimates in for short periods of time between clear-sky days. This approach may suffice on the point-scale, but may be less useful when a spatial analysis or interpretation is required.

Acknowledgments

Financial support for this work was supported by NASA Terrestrial Hydrology Program under Grant No. NNX15AB28G.

References

1. K. L. Brubaker and D. Entekhabi, "Analysis of feedback mechanisms in land-atmosphere interaction," *Water Resour. Res.* **32**(5), 1343–1357 (1996).
2. T. Delworth and S. Manabe, "The influence of soil wetness on near-surface atmospheric variability," *J. Clim.* **2**, 1447–1462 (1989).
3. R. A. Pielke, "Influence of the spatial distribution of vegetation and soils on the prediction of cumulus convective rainfall," *Rev. Geophys.* **39**(2), 151–177 (2001).
4. J. Shukla and Y. Mintz, "Influence of land-surface evapotranspiration on the earth's climate," *Science* **215**(4539), 1498–1501 (1982).
5. E. Njoku and D. Entekhabi, "Passive microwave remote sensing of soil moisture," *J. Hydrol.* **184**(1/2), 101–129 (1996).
6. T. Schmugge et al., "Remote sensing in hydrology," *Adv. Water Resour.* **25**(8-12), 1367–1385 (2002).
7. D. Entekhabi et al., "An agenda for land surface hydrology research and a call for the second international hydrological decade," *Bull. Am. Meteorol. Soc.* **80**(10), 2043–2058 (1999).
8. W. Wagner et al., "Operational readiness of microwave remote sensing of soil moisture for hydrologic applications," *Hydrol. Res.* **38**(1), 1–20 (2007).
9. S. Sanchez-Ruiz et al., "Combining SMOS with visible and near/shortwave/thermal infrared satellite data for high resolution soil moisture estimates," *J. Hydrol.* **516**, 273–283 (2014).
10. E. Njoku et al., "Soil moisture retrieval from AMSR-E," *IEEE Trans. Geosci. Remote Sens.* **41**(2), 215–229 (2003).
11. J. C. Calvet et al., "Sensitivity of passive microwave observations to soil moisture and vegetation water content: L-band to W-band," *IEEE Trans. Geosci. Remote Sens.* **49**(4), 1190–1199 (2011).
12. J. Y. Kim and T. S. Hogue, "Improving spatial soil moisture representation through integration of AMSR-E and MODIS products," *IEEE Trans. Geosci. Remote Sens.* **50**(2), 446–460 (2012).
13. T. J. Jackson et al., "Large area mapping of soil moisture using the ESTAR passive microwave radiometer in Washita '92," *Remote Sens. Environ.* **54**(1), 27–37 (1995).
14. T. J. Jackson et al., "Soil moisture mapping at regional scales using microwave radiometry: the Southern Great Plains hydrology experiment," *IEEE Trans. Geosci. Remote Sens.* **37**(5), 2136–2151 (1999).
15. Y. H. Kerr et al., "Soil moisture retrieval from space: the soil moisture and ocean salinity (SMOS) mission," *IEEE Trans. Geosci. Remote Sens.* **39**, 1729–1735 (2001).
16. Y. H. Kerr et al., "The SMOS mission: new tool for monitoring key elements of the global water cycle," *Proc. IEEE* **98**(5), 666–687 (2010).
17. Y. H. Kerr et al., "The SMOS soil moisture retrieval algorithm," *IEEE Trans. Geosci. Remote Sens.* **50**, 1384–1403 (2012).
18. Y. H. Kerr et al., "CATDS SMOS L3 soil moisture retrieval processor Algorithm Theoretical Baseline Document (ATBD)," Technical Note, SO-TN-CBSA-GS-0029, Issue 2.0, p. 73, CBSA, www.cesbio.ups-tlse.fr/SMOS_blog/wp-content/uploads/2013/08/ATBD_L3_rev2_draft.pdf (2013).
19. D. Entekhabi et al., "The soil moisture active passive SMAP mission," *Proc. IEEE* **98**(5), 704–716 (2010).
20. O. Merlin et al., "Assimilation of disaggregated microwave soil moisture into a hydrologic model using coarse-scale meteorological data," *J. Hydrometeorol.* **7**(6), 1308–1322 (2006).
21. J. Pellenq, Y. Kerr, and G. Boulet, "Scaling and assimilation of SMOS data for hydrology," in *Proc. IEEE Geosci. Remote Sens. Symp.*, Vol. 5, pp. 3064–3066 (2003).

22. N. Chauhan, S. Miller, and P. Ardanuy, "Spaceborne soil moisture estimation at high resolution: a microwave-optical/IR synergistic approach," *Int. J. Remote Sens.* **24**, 4599–4622 (2003).
23. O. Merlin et al., "A combined modeling and multispectral/multiresolution remote sensing approach for disaggregation of surface soil moisture: application to SMOS configuration," *IEEE Trans. Geosci. Remote Sens.* **43**, 2036–2050 (2005).
24. T. N. Carlson, R. R. Gillies, and E. M. Perry, "A method to make use of thermal infrared temperature and NDVI measurements to infer surface soil water content and fractional vegetation cover," *Remote Sens. Rev.* **9**(1–2), 161–173 (1994).
25. I. Sandholt, K. Rasmussen, and J. Anderson, "A simple interpretation of the surface temperature/vegetation index space for assessment of soil moisture status," *Remote Sens. Environ.* **79**(2/3), 213–224 (2002).
26. M. Hemakumara et al., "Downscaling of low resolution passive microwave soil moisture observations," in *2nd Int. CAHMDA Workshop on the Terrestrial Water Cycle: Modelling and Data Assimilation Across Catchment Scales*, Princeton, New Jersey, A. J. Teuling, Eds. et al., pp. 51–55 (2004).
27. A. Hossain and G. Easson, "Evaluating the potential of VI-LST triangle model for quantitative estimation of soil moisture using optical imagery," in *Proc. IEEE Geoscience Remote Sensing Symp.* (2008).
28. M. Piles et al., "Downscaling SMOS-derived soil moisture using MODIS Visible/Infrared," *IEEE Trans. Geosci. Remote Sens.* **49**(9), 3156–3166 (2011).
29. S. Jin et al., "A comprehensive change detection method for updating the National Land Cover Database to circa 2011," *Remote Sens. Environ.* **132**, 159–175 (2013).
30. B. Morelo et al., "SMOS disaggregated soil moisture product at 1 km resolution: processor overview and first validation results," *Remote Sens. Environ.* **180**, 361–376 (2016).
31. D. K. Adams and A. C. Comrie, "The North American monsoon," *Bull. Am. Meteorol. Soc.* **78**, 2197–2213 (1997).
32. M. H. Cosh et al., "Temporal persistence and stability of surface soil moisture in a semiarid watershed," *Remote Sens. Environ.* **112**(2), 304–313 (2008).
33. C. Zhu et al., "Evaluating the influence of antecedent soil moisture on variability of the North American monsoon precipitation in the coupled MM5/VIC modeling system," *J. Adv. Model. Earth Syst.* **1**, 1–22 (2009).
34. P. L. Nagler et al., "Relationship between evapotranspiration and precipitation pulses in a semiarid rangeland estimated by moisture flux towers and MODIS vegetation indices," *J. Arid Environ.* **70**(3), 443–462 (2007).
35. W. E. Emmerich, "Ecosystem water use efficiency in a semiarid shrubland and grassland community," *Rangeland Ecol. Manage.* **60**(5), 464–470 (2007).
36. T. J. Jackson et al., "Validation of advanced microwave scanning radiometer soil moisture products, *IEEE Trans. Geosci. Remote Sens.* **48**(12), 4256–4272 (2010).
37. R. Bindlish, "Global soil moisture from the aquarius/SAC-D satellite: description and initial assessment," *IEEE Geosci. Remote Sens. Lett.* **12**(5), 923–927 (2015).
38. D. J. Leroux, "Comparison between SMOS, VUA, ASCAT, and ECMWF soil moisture products over four watersheds in U.S.," *IEEE Trans. Geosci. Remote Sens.* **52**(3), 1–10 (2013).
39. T. J. Jackson, "Validation of soil moisture and ocean salinity (SMOS) soil moisture over watershed networks in the U.S.," *IEEE Trans. Geosci. Remote Sens.* **50**(5), 1530–1543 (2012).
40. J. P. Wigneron, "L-band microwave emission of the biosphere (L-MEB) model: description and calibration against experimental data sets over crop fields," *Remote Sens. Environ.* **107**, 639–655 (2007).
41. B. Hornbuckle and A. England, "Diurnal variation of vertical temperature gradients within a field of maize: implications for satellite microwave radiometry," *IEEE Geosci. Remote Sens. Lett.* **2**(1), 74–77 (2005).
42. A. R. Huete et al., "Global-scale analysis of vegetation indices for moderate resolution monitoring of terrestrial vegetation," *Proc. SPIE* **3868**, 141 (1999).
43. S. Chakrabarti et al., "Downscaling satellite-based soil moisture in heterogeneous regions using high resolution remote sensing products and information theory: a synthetic study," *IEEE Trans. Geosci. Rem. Sens.* **53**(1), 85–101 (2015).

44. A. M. Mood, F. A. Graybill, and D. C. Boes, "Introduction to the theory of statistics," in *McGrawHill Series in Probability and Statistics*, Vol. **3**, McGraw-Hill, California, http://www.librarything.com/work/1154157/book/32217714 (1974).
45. N. J. Salkind, "Standard error of the estimate," in SAGE, Ed., *Encyclopedia of Research Design*, Vol. **3**, pp. 1426–1430, SAGE Publications, Inc., London (2010).
46. D. Entekhabi, "Performance metrics for soil moisture retrievals and application requirements," *J. Hydrometeorol.* **11**, 832–840 (2010).
47. O. Merlin, "Towards deterministic downscaling of SMOS soil moisture using MODIS derived soil evaporative efficiency," *Remote Sens. Environ.* **112**, 3935–3946 (2008).
48. O. Merlin, "Disaggregation of SMOS soil moisture in Southeastern Australia," *IEEE Trans. Geosci. Remote Sens.* **50**, 1556–1571 (2012).
49. O. Merlin, "Self-calibrated evaporation-based disaggregation of SMOS soil moisture: an evaluation study at 3 km and 100 m resolution in Catalunya, Spain," *Remote Sens. Environ.* **130**, 25–38 (2013).

Kyle R. Knipper received his BS degree in meteorology from Iowa State University and his MS degree in hydrologic science and engineering from Colorado School of Mines in 2013 and 2015, respectively. He is a PhD student at the Colorado School of Mines. His current research interests include the development and application of remotely sensed products, evapotranspiration and soil moisture dynamics, and hydrologic and atmospheric model applications of remotely sensed data, with a focus in dynamic environments undergoing acute or chronic disturbances.

Terri S. Hogue is a professor in the Department of Civil an Environmental Engineering at the Colorado School of Mines. She received her PhD from the Department of Hydrology and Water Resources at the University of Arizona. Her research focuses on understanding hydrologic and land surface processes, with an emphasis on human interactions with water cycling and management. Projects include wildfire impacts, urbanization and ecosystem dynamics, and hydrologic response to climate change.

Kristie J. Franz is an associate professor in the Department of Geological and Atmospheric Sciences at Iowa State University. She received her PhD in civil engineering from the University of California, Irvine. Her work focuses on advancing hydrologic modeling and prediction systems for short to long time horizons. Recent projects include investigating satellite-based observations and ensemble precipitation forecasts for streamflow forecasting, and improving representation and assessment of human influences on hydrologic processes through agent-based modeling.

Russell L. Scott is a research hydrologist for the USDA-ARS in Tucson, Arizona. His research concerns the exchanges of energy, water and carbon dioxide at the soil, vegetation, and atmospheric interface and the interactions between hydrology and ecology in water-limited areas.